NeuroImage 56 (2011) 2047–2057

Contents lists available at ScienceDirect

NeuroImage

journal homepage: www.elsevier.com/locate/ynimg

An improved method for mapping cerebrovascular reserve using concurrent fMRI and near-infrared spectroscopy with Regressor Interpolation at Progressive Time Delays (RIPTiDe)

Yunjie Tong [a,b], Peter R. Bergethon [c,d], Blaise deB. Frederick [a,b,*]

[a] Brain Imaging Center, McLean Hospital, 115 Mill Street, Belmont, MA 02478, USA
[b] Department of Psychiatry, Harvard University Medical School, Boston, MA 02115, USA
[c] Department of Anatomy and Neurobiology, Boston University School of Medicine, Boston, MA 02118, USA
[d] Department of Biochemistry, Boston University School of Medicine, Boston, MA 02118, USA

ARTICLE INFO

Article history:
Received 5 October 2010
Revised 17 March 2011
Accepted 25 March 2011
Available online 1 April 2011

Keywords:
Cerebrovascular reserve
Near-infrared spectroscopy
Functional magnetic resonance imaging
Breath holding

ABSTRACT

Cerebrovascular reserve (CVR) reflects the compensatory dilatory capacity of cerebral vasculature to a dilatory stimulus. Blood oxygen-level dependent (BOLD) fMRI has been proven to be an effective imaging technique to obtain CVR maps when subjects perform CO_2 inhalation or a breath-holding (BH) task. Here we propose a novel way to process the fMRI data obtained during a blocked BH task by using simultaneously collected near-infrared spectroscopy (NIRS) data as regressors to estimate the vascular contribution to the BOLD signal.

Six healthy subjects underwent a 6 min 30 s resting state (RS) fMRI scan, followed by a scan of the same duration with a blocked BH task (5 breath holds with 20 s durations separated by ~50 s of regular breathing). NIRS data were recorded from a probe over the subjects' right prefrontal area. For each scan, the time course of changes in total hemoglobin (Δ[tHb]) was calculated from the NIRS data, time shifted by various amounts, and resampled to the fMRI acquisition rate. Each shifted time course was used as regressor in a general linear model analysis. The maximum parameter estimate across all time shifts was calculated at all voxels in both the BH and RS scans, and then converted into signal percentage changes. The ratio of these signal changes generates a CVR map of the BH response, normalized to the resting state. The NIRS regressor method makes no assumptions about the shape (or presence) of the BH response, and allows direct, quantitative comparison of the vascular BOLD response to BH to the baseline map obtained in the resting state.

Introduction

Brain health requires that the cerebral vasculature be able to supply an appropriate amount of oxygen and nutrients to brain tissue under a wide range of physiological conditions. These conditions include both the normal resting baseline state (resting state, "RS"), and states with higher oxygen requirements; to meet this requirement, the vasculature undergoes autoregulatory vasodilation to respond to increased demand. Cerebrovascular reserve (CVR) is a measure that reflects the capacity for vasodilation and is an indicator of vascular reserve in the brain. The CVR map may offer useful clinical information in patients at risk for cerebral ischemia associated with chronic stenosis or occlusion of the large cerebral blood vessels (Mandell et al., 2008; Pindzola et al., 2001; Vernieri et al., 1999; Ziyeh et al., 2005). The CVR is also a potential marker for risk of ischemia to the deep white matter, which leads to sub-cortical infarction (Bakker et al., 1999; Cupini et al., 2001; Vernooij et al., 2008) and may reflect abnormalities in diabetes (Kozera et al., 2009), and dementing illnesses including Alzheimer's disease (Yezhuvath et al., 2010). The assessment of CVR commonly involves maneuvers that increase the cerebral CO_2, such as inhaled CO_2 or an intravenous acetazolamide challenge, which both act as potent stimuli for vasodilation (Driver et al., 2010; Lythgoe et al., 1999). Breath holding ("BH") has been shown to be an effective alternative method for perturbing cerebral CO_2 concentration (Corfield et al., 2001; Kastrup et al., 1999a; Kastrup et al., 1999b; Li et al., 1999; Liu et al., 2002; Magon et al., 2009) that also increases the CO_2 level in the blood stream, and has been proved to be equally effective in the evaluation of the CVR map as CO_2 inhalation (Kastrup et al., 2001). An additional advantage of BH is that the BH method is simpler and noninvasive.

Functional magnetic resonance imaging (fMRI) based on blood oxygen-level dependent (BOLD) contrast has been successfully used to generate cerebrovascular response and/or reactivity maps using either CO_2 inhalation (Lythgoe et al., 1999; van der Zande et al., 2005; Yezhuvath et al., 2009) or breath holding (Kastrup et al., 2001; Li et al., 1999; Magon et al., 2009). The general approach is to acquire BOLD-

* Corresponding author at: Brain Imaging Center, McLean Hospital, 115 Mill Street, Belmont, MA 02478, USA. Fax: +1 617 855 2770.
E-mail address: bbfrederick@mclean.harvard.edu (B. Frederick).

1053-8119/$ – see front matter © 2011 Elsevier Inc. All rights reserved.
doi:10.1016/j.neuroimage.2011.03.071

sensitive images while the subject either breathes air with elevated CO_2 concentrations (5–10% CO_2) or is asked to hold his/her breath in a block-design manner. The increased CO_2 induces vasodilation, which in turn increases cerebral perfusion, providing sufficient additional oxy-hemoglobin to the area to increase local blood oxygenation, increasing the BOLD signal amplitude. To calculate the CVR map obtained from fMRI, voxelwise correlation of BOLD signal with a boxcar function representing the stimulus protocol is commonly used. However, there are several drawbacks in using the boxcar function. First, the hemodynamic latency must be empirically estimated (Goode et al., 2009; Kastrup et al., 2001). Magon et al. (2009) proposed a more accurate method which involved performing a prior exploratory analysis to determine the average latency. However, neither of these whole-brain methods is highly accurate since the hemodynamic latency may change over time from block to block. Secondly, it has been shown that the vascular latencies differ across the brain (Chang et al., 2008; Handwerker et al., 2004; Thomason et al., 2005). Spatial variability may be accounted for by regional differences in coupling between neuronal activity and vascular response, large vessel effects (Lee et al., 1995) and vasculature differences (Miezin et al., 2000). A single boxcar regressor, even when combined with the first derivative of the hemodynamic response function, is not adequate to analyze regional differences in latencies if these differences are greater than ~2 s (Handwerker et al., 2004). Moreover, the boxcar function itself does not account for the variation in the strength of the BOLD response over the course of the breath-holding period as arterial CO_2 increases; the boxcar, even convolved with a hemodynamic response function, is likely to poorly model the actual response.

Murphy et al. (2011) have recently developed an improved analysis method for breath hold BOLD scans which more closely models the shape of the response to breath holding, and accounts for the accumulation of CO_2 in the bloodstream over the course of an experiment by using a model waveform derived from the measured EtCO2. This method provides a significant improvement over the boxcar regressor model, accounting for a good deal more of the variance over the whole head. However, this analysis method still makes two assumptions regarding the response shape; the first is that a simple linear extrapolation of the CO_2 across the breath-holding period adequately models the response shape, and the second is that the spatial variability in response delay is fully accounted for through the use of a time derivative.

Here we propose an alternative method for obtaining the response to a breath hold, using a concurrent NIRS measurement to obtain both the physiological response to the breath hold and the appropriate voxelwise time delay directly. This technique has the advantage that it makes no assumptions at all about the response shape or the perturbing stimulus, and works equally well without a breath hold, allowing direct comparison of breath hold and resting state data.

Several concurrent NIRS and fMRI studies have been published (Huppert et al., 2006; Sassaroli et al., 2006; Strangman et al., 2002; Toronov et al., 2001), which have provided evidence supporting the high temporal correlation between BOLD and NIRS signals in task activations. MacIntosh et al. (2003) studied transient hemodynamics during a BH challenge using concurrent NIRS and fMRI and found a strong linear relationship between transverse relaxation rate (R_2^*) and absolute deoxy-hemoglobin. In our previous concurrent NIRS/fMRI studies during the resting state, we were able to generate a map of the vascular component of the BOLD signal in the resting brain by tracking the low frequency oscillations throughout the brain (Tong and Frederick, 2010).

In this concurrent NIRS and fMRI study, we used the total hemoglobin concentration changes calculated from NIRS as a regressor in a general linear model (GLM) to analyze the BOLD signals obtained during both a BH task and an RS scan. Our hypothesis is that since both the BOLD and NIRS signals arise as a consequence of the same hemodynamic mechanisms (variations in blood volume and oxygenation), the changes in the hemoglobin calculated using the NIRS signal as a regressor would be a more accurate match to the BOLD data than the simple convolved block diagram. Most importantly, using the proper, voxel-specific delay between the NIRS regressor and the BOLD data would accurately compensate for temporal variation in the vascular latency over the course of the experiment, which are not accounted for when using the block diagram. Therefore, we applied the method demonstrated in our previous work (Tong and Frederick, 2010) by using time-shifted NIRS regressors to model the physiological signal in voxels activated at different time lags and then combine them to produce a more accurate and thorough CVR map (non-normalized).

In order to normalize the CVR, by controlling for baseline differences in hemoglobin concentration, the parameter estimates (PE) of the BOLD response to the Δ[tHb] NIRS regressor at the voxel-specific time delay were converted to signal percentage changes in both cases (BH and RS) and the ratio was calculated to obtain the normalized CVR map. As a result, we found that 1) the largest changes (>20%) occur in large blood vessels (mainly drainage veins) in both cases and 2) large signal changes (>1.5%) were observed in much broader areas within the gray matter during BH tasks, presumably due to vessel dilation caused by elevated CO_2 level in the blood.

Materials and methods

Protocol

A concurrent NIRS and fMRI study was conducted on 6 healthy volunteers (4 M, 2 F, aged 28.0 ± 4 years). Informed consent was obtained prior to scanning. The protocol was approved by the Institutional Review Board at McLean Hospital. Two functional MRI scans of same length (6 min 30 s) were performed on each subject in the same session separated by a brief interval, an RS scan, followed by a BH scan. During the RS scan, the participants were asked to lie quietly in the scanner while viewing a gray screen with a central fixation point. During the BH scan, the task was the same for most of the period, but the subject was additionally asked 5 times during the scan to hold their breath after natural expiration for a period of 20 s. Between the BH periods, the subject was given resting times of different lengths (40, 50, 50, and 60 s). Three seconds before the beginning of the BH period, the subjects were presented with a countdown clock at the center to cue them. During the BH period, the subject viewed a gray screen with the words “Hold the Breath” in the center and a countdown clock at the upper-left corner indicating the number of seconds left for the BH. The visual displays were generated using Psychtoolbox (Brainard, 1997).

fMRI acquisition and physiological monitoring

All MR data were acquired on a Siemens TIM Trio 3T scanner (Siemens Medical Systems, Malvern, PA) using a 12-channel phased array head matrix coil. A high-resolution anatomic image set was acquired for slice positioning and coregistration of the functional data (T1 weighted multiecho MP-RAGE3D (van der Kouwe et al., 2008), resolution (RL, AP, SI) of 1.33 × 1 × 1 mm, TI = 1100 ms, TR/TE1, TE2 = 2530/3.31, 11.61 ms, FOV = 171 × 256 × 256 mm, 128 × 256 × 256 pixels, 2× GRAPPA, total imaging time 4 min 32 s). This was followed by the RS and BH fMRI scans with identical parameters (gradient echo EPI acquisitions with prospective motion correction (PACE), 2 dummy shots, 260 time points, TR/TE = 1500/30 ms, flip angle 75 degrees, matrix = 64 × 64 on a 220 × 220 mm FOV, 29 3.5 mm slices with 0.5 mm gap parallel to the AC-PC line extending down from the top of the brain, GRAPPA acceleration factor of 3). Physiological waveforms (pulse oximetry and respiratory depth) were recorded using the scanner's built-in wireless fingertip pulse oximeter and respiratory belt.

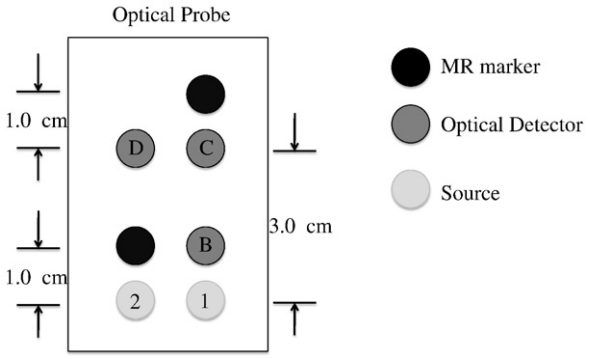

Fig. 1. Schematic diagram of the optical probe.

NIRS acquisition

NIRS data were collected by means of an MRI compatible NIRS probe placed on each participant's forehead over the right prefrontal area (roughly between Fp1 and F7 in the 10–20 system) and held in place by an elastic band around the head. The position of the probe was chosen due to its easy accessibility (directly on the forehead) and relatively short distance from the skin surface to the cortex (11–13 mm on average) in this area (Okamoto et al., 2004). The probe consisted of three collection and two illumination optical fibers, with source-detector distances of 1 or 3 cm (see Fig. 1) embedded in a soft plastic sheet along with MRI-visible markers to identify the probe location on the anatomic MRI images. Fig. 1 is a diagram of the probe showing the arrangement of MRI-visible markers as well as the illumination and collection fibers on the NIRS probe. Each illumination fiber delivered light from two laser diodes emitting at wavelengths of 690 and 830 nm. The laser diodes and three optical detectors (photomultipliers tubes, Hamamatsu Photonics R928) were housed in a near-infrared tissue imager (Imagent, ISS, Inc., Champaign, IL), which was placed in the MRI control room. The optical probe and the Imagent instrument were connected by 10 m long optical fibers. The sampling rate of NIRS data acquisition was 12.5 Hz. fMRI data were collected for 6 min 30 s; NIRS data were recorded continuously during this time as well as for several minutes before and after the fMRI acquisition.

NIRS and fMRI data analysis

In order to evaluate the performance of the new analysis technique, the data were analyzed twice. The data were first analyzed in the conventional manner, using a boxcar function as the regressor to map the activated voxels. The data were then reanalyzed using regressors obtained from NIRS data. The results were compared to each other. In order to compare the maps during RS and BH period, the procedure that used the NIRS data as regressors was also applied on the RS fMRI data. All fMRI data processing was performed using FEAT, part of the FSL analysis package (FMRIB Expert Analysis Tool, v5.98, http://www.fmrib.ox.ac.uk/fsl, Oxford University, UK) (Smith et al., 2004).

Boxcar regressor

First, we processed the BH data using conventional methods by using the block diagram of the BH periods as the regressor of interest. To estimate the hemodynamic latency, we used the method proposed by Magon et al. (2009) to determine the "best" time shift for the boxcar. In this process, a cross-correlation analysis was conducted between a boxcar function and the BOLD signal. The result indicated the time shift at which the maximal correlation was produced. This procedure was carried out for all the voxels in a gray matter ROI and the averaged time shift that produced maximum correlation was calculated. This value was then used to shift the boxcar function (after convolution with the double-gamma function) to get the "temporally adjusted regressor" (as seen in Fig. 2(b)), that is used in the GLM later. A 3-D thresholded *z*-statistic map (CVR map) was created as the result of the analyses.

NIRS regressor

A novel procedure was used to create the CVR maps using simultaneous NIRS data as a regressor, based on a refinement of our previously described concurrent processing method (Tong and Frederick, 2010). Each pair of raw NIRS time courses (690 and

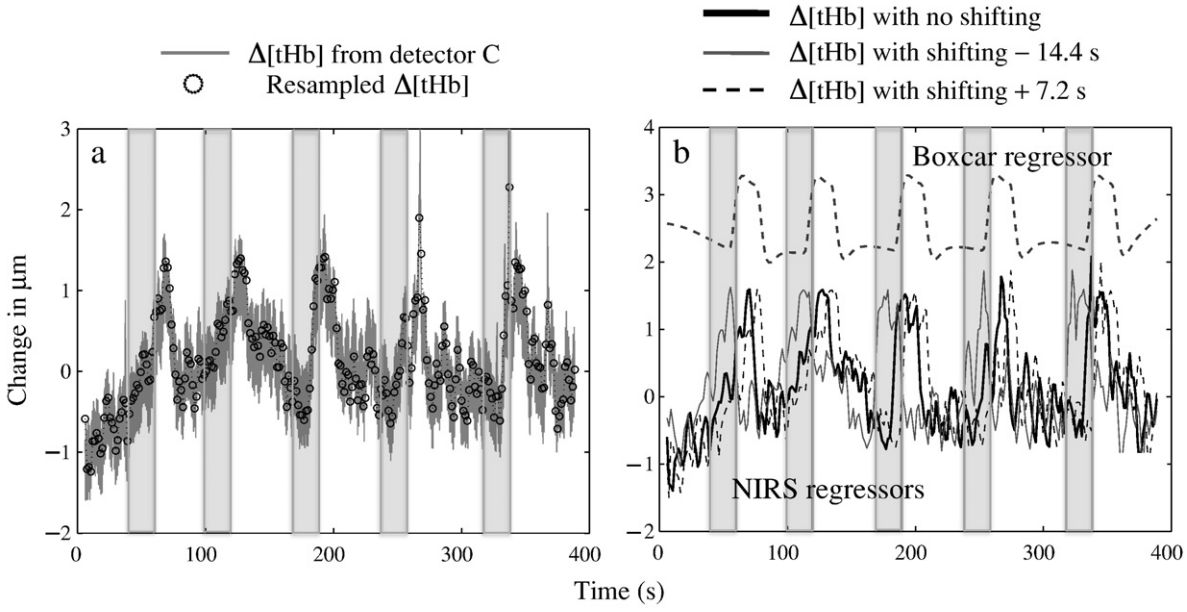

Fig. 2. (a) Temporal trace of the original Δ[tHb] (gray line) NIRS data from subject 3 calculated from C1, with the resampled Δ[tHb] time points superimposed (black circles). The BH periods are indicated by the shaded areas. (b) Temporally adjusted boxcar regressor convolved with double-gamma function (top) and 3 representative regressors of various time shifting used in the study from Δ[tHb].

830 nm data) was converted into two time courses representing temporal changes of the concentrations of oxy-hemoglobin (Δ[HbO]) and deoxy-hemoglobin (Δ[Hb]) according to the differential path length factor method (Matcher, 1994) using a Matlab program (The MathWorks, Natick, MA). The change of concentration of total hemoglobin (Δ[tHb]) was calculated by adding Δ[HbO] and Δ[Hb] together. The data from path C1 (Fig. 1) were chosen due to the high signal to noise ratio (SNR) for all the subjects. The time courses of Δ[tHb] were then anti-aliased and down-sampled to the fMRI acquisition frequency of 0.67 Hz (1/1.5 s), which was 260 data points. Fig. 2(a) shows the temporal traces of Δ[tHb] (gray) measured from path C1 on an example subject (subject 3) and the corresponding resampled Δ[tHb] data (black circle). The down-sampled Δ[tHb] data were later used as regressors in the GLM analysis of the BOLD data. The rationale for using Δ[tHb] is discussed below.

Voxelwise estimation of optimal regressor time delay

There are two factors which make the method of Magon et al. (2009) unsuitable for estimating the optimal delay for the NIRS regressor. The first, as we mentioned before, is that the method relies on having a relatively simple boxcar waveform to estimate the time-to-peak in the complex BOLD data. Second, we want to determine the optimal delay on a voxelwise, rather than ROI-wise basis, so we do not get the SNR benefit of averaging over a large region of tissue.

The most straightforward method for determining the optimal delay is to calculate the voxelwise cross-correlation between the resampled NIRS signal and the BOLD data, and then find the peak time lag value. In practice this does not work well; the resulting cross-correlation is quite noisy, the peak is broad, and there is no way to account for confounds such as motion. A better but more computationally intensive way to perform this estimation is to perform a full GLM analysis on the data many times in FSL, with each analysis differing only in the time shift of the NIRS regressor, taking advantage of FSL's ability to covary out confound regressors and prewhiten the BOLD signal. The peak response is then found for each voxel in the image. We refer to this analysis method as Regressor Interpolation at Progressive Time Delays (RIPTiDe).

We implemented this by applying a range of time shifts to the NIRS signal prior to resampling. A positive time shift value means that the resampled waveform corresponds to events that happened prior to the time the NIRS data were recorded. Because of the high temporal resolution of NIRS acquisition (12.5 Hz), the shifting step can be as small as 0.08 s. However, in this particular study, due to the fact that TR was 1.5 s, we found that 0.24 s was a small enough step to catch all the subtle changes in BOLD signals. We considered 91 time shift values covering the range of −14.4 to 7.2 s (at a step of 0.24 s) with respect to the unshifted signal. The time limits were determined as the result of a preliminary analysis to find the time shift range over which significant correlations were observed. Fig. 2(b) shows a subset of 3 of the 91 regressors (from Δ[tHb]) with time shifts of −14.4, 0 and +7.2 s, respectively. The image analysis was repeated 91 times on the fMRI data collected during BH—once for each of the time-shifted NIRS Δ[tHb] regressors (we note that this time delay estimation step is simply an implementation detail, and does not therefore require Bonferroni correction for multiple comparisons).

The resulting thresholded *z*-statistic maps were concatenated in time and the final step involved finding the maximum *z* value along the time course of each voxel; this corresponds to the optimal regressor time delay for that voxel. We then formed a new 3-D image

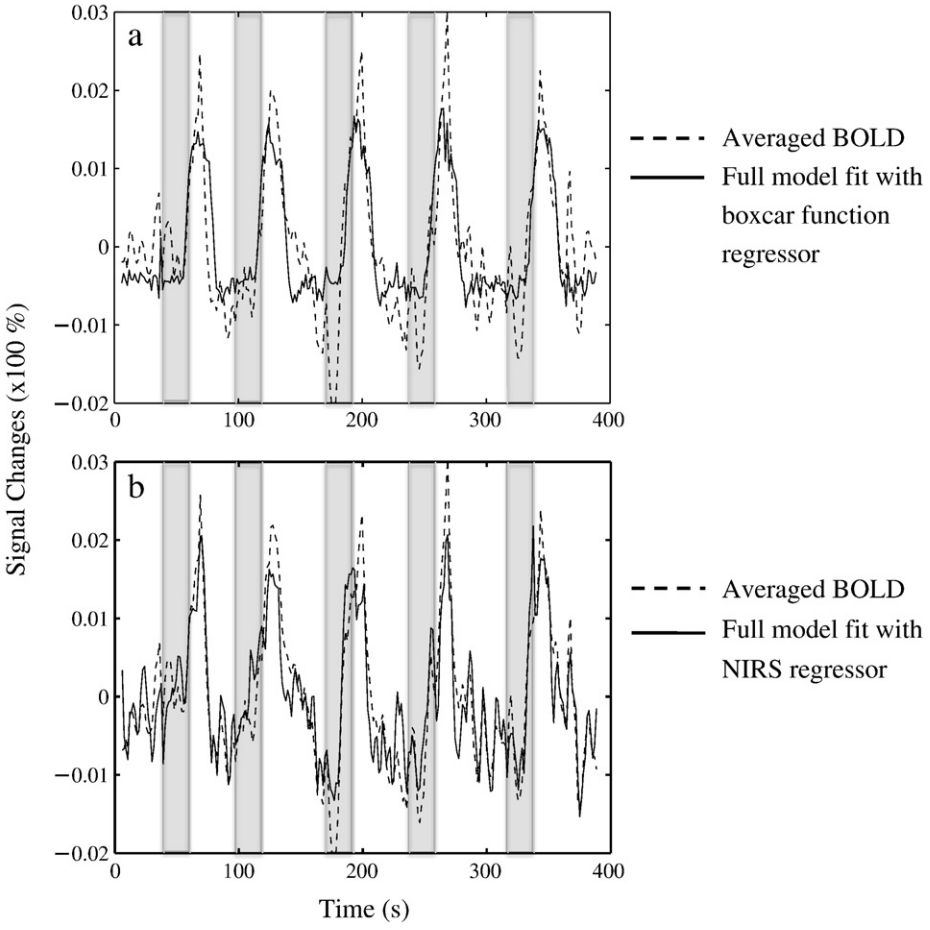

Fig. 3. Averaged BOLD signals and the full-model fit from using boxcar function (a) and fixed NIRS regressor (b). The BH periods are indicated by the shaded areas.

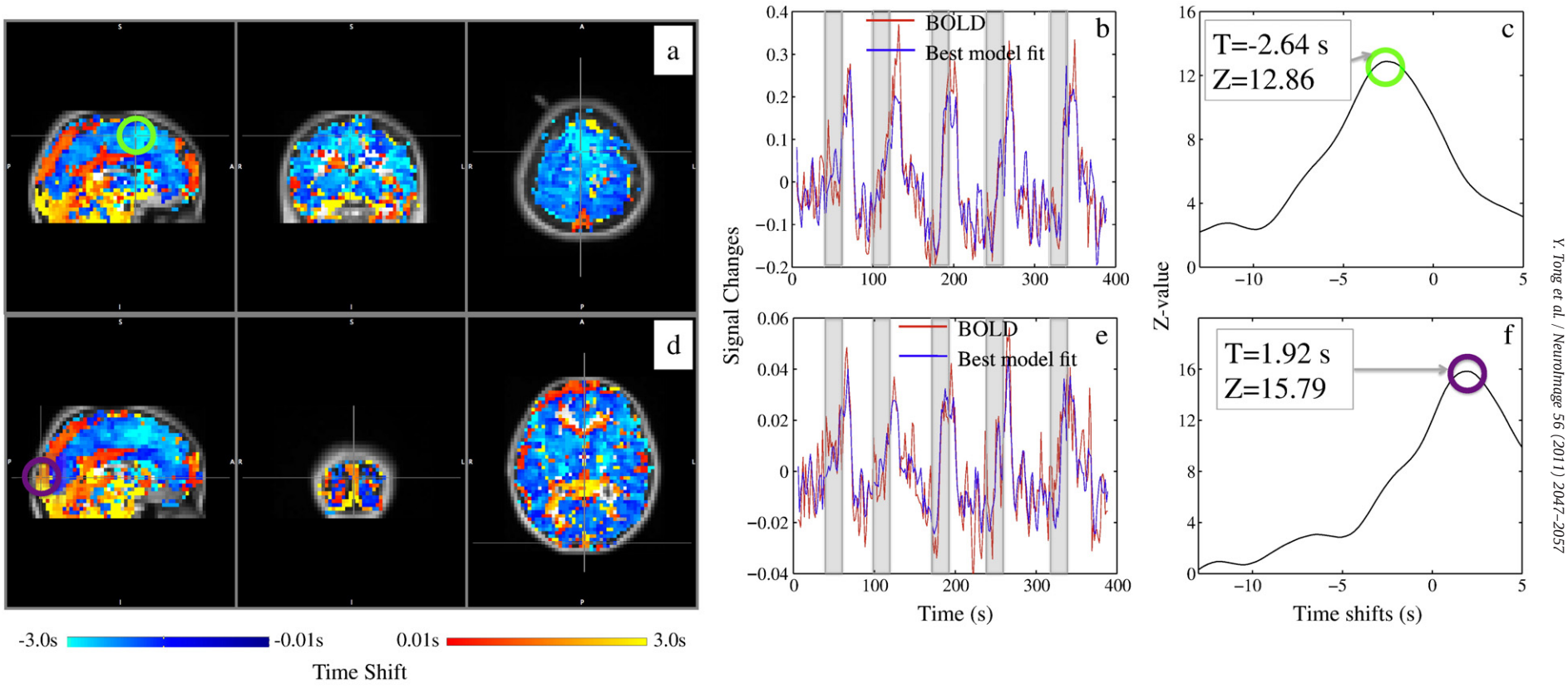

Fig. 4. (a) and (d) Optimum regressor time lag map (obtained by finding the time shift with maximum *z* value for each voxel) of subject 3 overlaid the structural brain. The green circle in (a) indicates the voxel from which the BOLD signal and its corresponding full-model fit are shown in (b). The plot of *z* value vs. time shift of the NIRS regressor for the same voxel (green) is shown in (c). The purple circle indicates the voxel from which the BOLD signal and its corresponding full-model fit are shown in (e), the plot of *z* value vs. time shift for the same voxel (purple) is shown in (f).

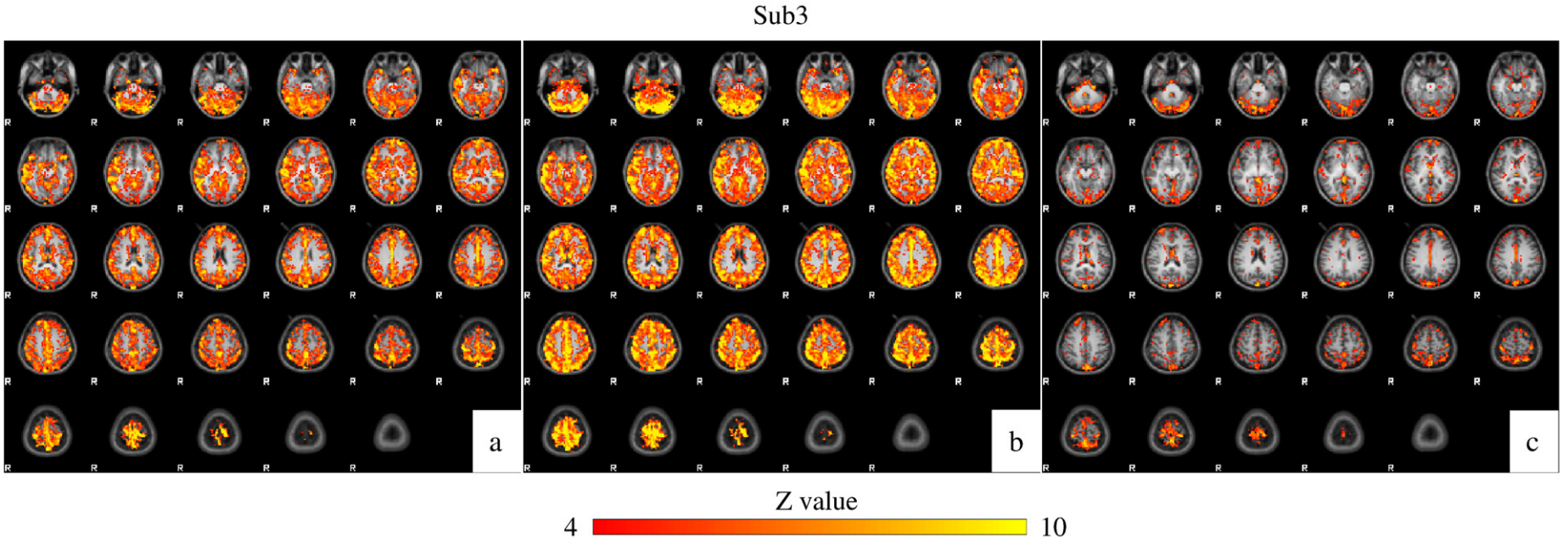

Fig. 5. Thresholded maximum *z*-statistic maps (non-normalized CVR map) of subject 3 using a boxcar function as regressor in BH (a), shifted NIRS Δ[tHb] as regressors in BH (b) and in RS (c).

(the non-normalized CVR map) from these z values. This CVR map was then registered onto the subject's structural scan, then the MNI152 standard head. The identical procedure was then performed on the RS fMRI data for comparison of the number of activated voxels.

For quantitative comparison of activation strength between states (BH and RS) in each voxel, we compared the PE for the response (expressed as percentage signal change) at the optimal regressor time delay determined in the previous step.

fMRI data analysis parameters

Detailed fMRI preprocessing steps included motion correction (Jenkinson and Smith, 2001), slice time correction, spatial smoothing (Gaussian kernel of full-width-half-maximum = 5 mm) and high pass temporal filtering (cut-off frequency = 0.01 Hz to remove very slow instrumental drifts).

For each analysis, a temporal high pass filter (0.01 Hz) was applied to the NIRS regressor for consistency. The motion parameters, estimated from the motion correction preprocessing step on the fMRI data, were included as confounds to further remove motion-correlated noise.

The GLM was calculated voxel by voxel using FMRIB's improved linear model (FILM) with prewhitening (Woolrich et al., 2001). Regression coefficients at each voxel were transformed to z statistics, which indicated the statistical significance of model-related BOLD signal change. The significance threshold at the voxel level was set as $z>2.3$. A cluster threshold of $p<0.05$ was applied to the clusters which survived the local voxel threshold, and the significance of the cluster was computed.

Results and discussion

All the subjects but one were able to follow the instructions and hold their breaths accordingly without difficulties. One subject apparently fell asleep at the beginning of the BH and missed 2 out of 5 BH cues; the data from this subject were excluded from further analysis.

The use of Δ[tHb] as a regressor

In our previous work, we examined the use of the Δ[HbO] and Δ[Hb] signals to track blood moving through the brain. In this study, we are interested in the vasodilatory response to a BH challenge, so we are most interested in the cerebral blood volume (CBV) changes associated with the challenge. It has previously been established that changes in Δ[tHb] measured with NIRS correspond directly to changes in CBV (Emir et al., 2008; Vernieri et al., 2004). Because the ΔCBV (Δ[tHb]) waveform appears explicitly in models of the BOLD effect (Buxton et al., 1998), we felt that this was the most appropriate NIRS measure to use for estimating CVR. In practice, since the HbO concentration in cerebral blood is much higher than that of Hb (O_2 saturation is typically from 70–100%), the Δ[HbO] and Δ[tHb] signals are almost identical, and give very similar results.

Advantages of using NIRS regressors

Fig. 3 compares the results of analyses using each regressor described above for the example subject. The averaged temporal traces and the averaged full-model fits for all the voxels with statistically significant activations using the boxcar regressor are shown in Fig. 3(a). Fig. 3(b) shows the same data using one NIRS Δ[tHb] regressor (time shift: 0 s). By visual inspection, it is clear that the fixed NIRS regressor matched the BOLD signal more closely throughout the time course and particularly during the resting periods sandwiched by the BH periods. This is unsurprising, as the NIRS data are direct measurements of the changes in the hemoglobin concentration that are the source of BOLD signal. This helps in the following ways: 1) since NIRS directly measures the hemodynamic response to the BH, it is not necessary to assume or estimate a hemodynamic response, which is needed when using a boxcar regressor; 2) the hemodynamic response to BH may change from one BH period to another due to the adaptive nature of brain function and other physiological variables that influence the carbon dioxide retention caused by breath holding (this can be seen in Fig. 3). These changes are naturally reflected in the NIRS measurement, but not in the fixed-width boxcar function; 3) during the resting periods and the BH periods, there are spontaneous low frequency hemodynamic fluctuations (around 0.1 Hz), which are measured by NIRS (and improve the fit) and are not accounted for when using the boxcar function.

The NIRS measurement reflects the hemodynamic response to BH accurately and correlates with most of the activated voxels in the brain. Our previous work (Tong and Frederick, 2010) shows that the optimal time shift between the NIRS waveform (from the frontal lobe) and the BOLD signal varies throughout the brain. The variation in the time shifts closely follows the passage of blood circulating through the brain. Blood circulating through the body has variable levels of oxygenation; as this blood flows through the cerebrovascular circulatory system this oxygenation will cause the BOLD signal to vary throughout the brain with a similar pattern but variable delays depending on its arrival time. Fig. 4 is the optimum regressor time shift map for the example subject. The map was obtained from the concatenated z-statistic maps by taking the time index (in seconds) of the maximum z value over time for each voxel. In other words, the value in each voxel represents relative arrival times of the blood variation between that location and the site where the NIRS data were recorded (in the frontal area). In Fig. 4(a) and (d), we can see: 1) the patterns in blue represent the area that the blood arrived at before it reached the NIRS recording site; the blood reached the cerebral artery rich area (light blue) in the middle prior to the gray matter (deep blue); 2) the pattern in red and yellow represents the area that the blood propagated to after it reached the NIRS recording site; the largest delays occur in several big drainage veins (red and yellow). To further demonstrate the difference in arrival time among voxels, two voxels (marked by the green circle and the purple circle in Fig. 4(a) and (d)) from the same subject were chosen. Their BOLD signals and the full-model fits with the corresponding shifted NIRS regressors are shown in Fig. 4(b) and (e). The z values from each shifted NIRS regressor vs. time shift are shown in Fig. 4(c) and (f). The temporal traces (red) in Fig. 4(b) and (e) clearly indicate the existence of the delays in the hemodynamic response to the BH. This is further illustrated in Fig. 4(c) and (f), where the highest values of the z statistic are obtained by using the NIRS regressor shifted forward 2.64 s for one voxel (green) and backward 1.92 s for the other voxel (purple), respectively. This clearly indicated

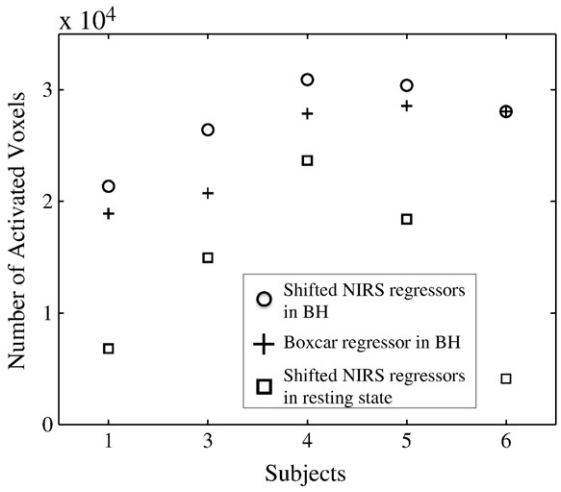

Fig. 6. Total number of activated voxels from 5 subjects obtained from using shifted NIRS regressors from BH (circle) and RS (square), while the cross shows the same result by using the boxcar regressor from BH.

that the time of maximum correlation between the NIRS and BOLD signals is spatially specific. Finally, the first voxel (green) in Fig. 4(a) was in the gray matter, while the second voxel (purple) in Fig. 4(d) was in the drainage vein (superior sagittal sinus); this directly affected the signal size, shown in Fig. 4(b) and (e). The signal changes are about 4% and 30%, respectively, indicating the much stronger signal changes in the big blood vessels, especially the veins. Fig. 4 confirms the necessity of using shifted NIRS regressors to optimally match all the voxels that are correlated with BH throughout the brain. The number of voxels detected by using the variably shifted NIRS regressor analysis increased by 23% when compared to the results of the boxcar regressor analyses.

Comparison between the results from NIRS regressors and boxcar regressor

Fig. 5 shows the thresholded *z*-statistic maps of the example subject (overlaid on the structural scan of the subject's own brain) obtained using the boxcar regressor (Fig. 5(a)) and the time-shifted NIRS regressors (Fig. 5(b)) in BH. A much more extensive CVR map (non-normalized) was obtained by using the shifted NIRS regressors. The results from the other subjects confirmed the finding. Fig. 6 shows the number of voxels detected by the different analysis methods for each subject (circles for shifted NIRS regressors and crosses for boxcar regressor). In all but one subject, shifted NIRS regressors detected visibly more meaningful voxels when compared to the boxcar regressor (12.5% more on average).

Comparison between the results from RS and BH

We previously demonstrated that by using shifted NIRS regressors in the analysis of resting state fMRI data we could map and track the blood oxygenation variations through the cerebral vasculature in the resting state (Tong and Frederick, 2010). This current study uses the same fMRI and NIRS acquisition parameters and processing steps, only differing in the addition of the BH task. Therefore, it is possible to directly compare the cerebrovascular function during the normal condition (RS) with that under the "stressed condition" evoked by

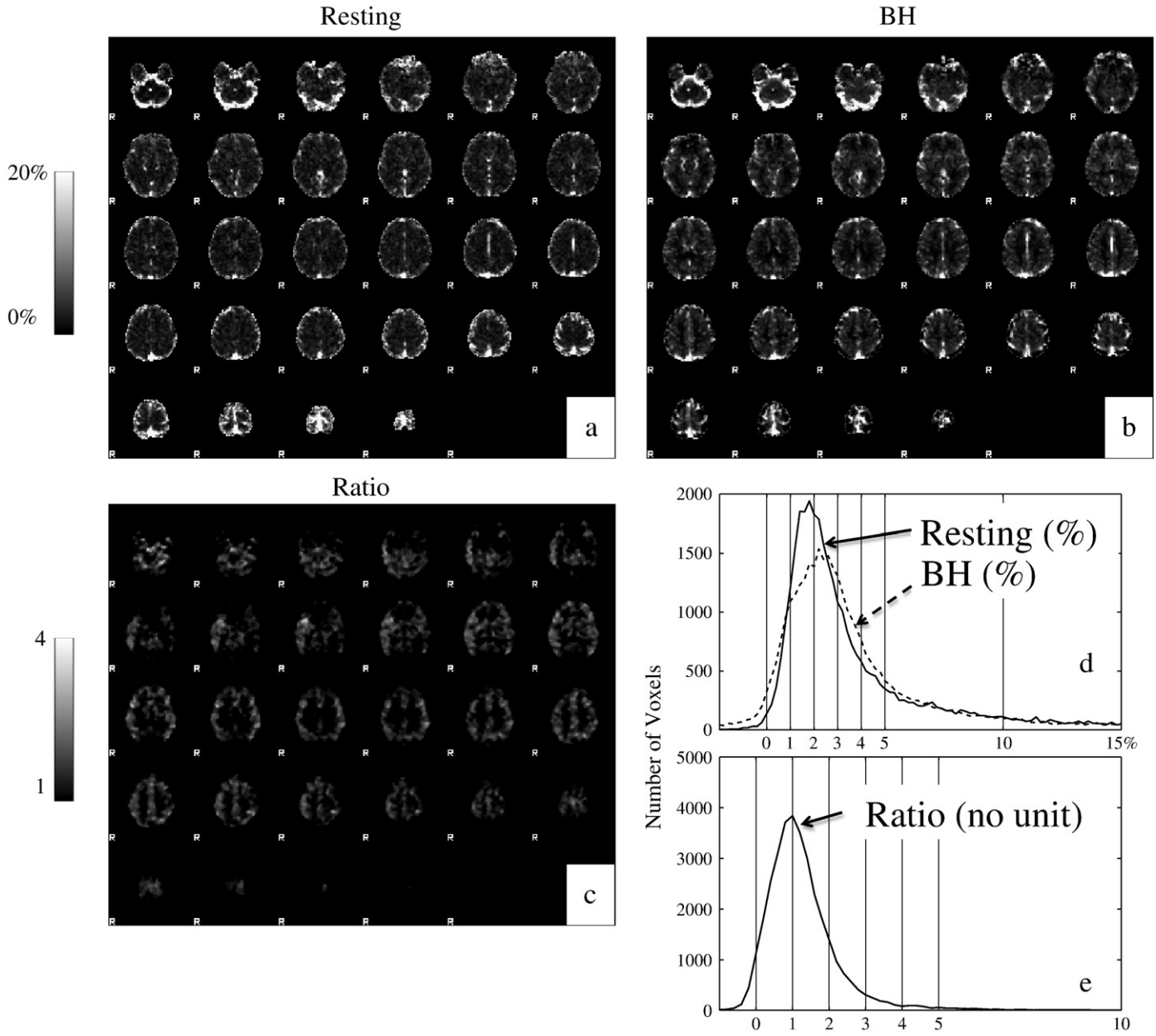

Fig. 7. The maps of BOLD percentage signal change of subject 3 for RS (a), BH (b) and the ratio between them (c). (d) Distribution of the voxels based on their signal changes in BH (dotted line) and RS (solid line). (e) Distribution of the voxels based on the ratio between BH and RS calculated at each voxel.

increased blood CO_2 levels (the BH scan). Fig. 5(b) shows the thresholded *z*-statistic map of BH (non-normalized CVR map) on the example subject using variably shifted NIRS regressors, while Fig. 5(c) shows the thresholded *z*-statistic map of RS on the same subject using the same method. It is clear by comparing these two graphs that the spatial distribution of activated voxels in Fig. 5(b) was much broader than that of Fig. 5(c), which is expected since increased CO_2 levels dilate the blood vessels and employ the blood reserve. Fig. 6 shows the number of activated voxels in RS (square) vs. BH (circle) for all the subjects. For all the subjects, more voxels were activated in the BH. Among them, subjects 1 and 6 had the largest increases in voxel numbers from RS to BH, while subject 4 had the least change. This subject-specific difference may be the consequence of differences in the capacity of vessels to dilate among subjects as well as variability among subjects in the degree of hypercapnia attained with the breath-holding exercise, or variations in the baseline hemoglobin concentrations. In order to normalize out baseline hemoglobin effects, we must combine the measurements.

In order to compare the two conditions quantitatively, the NIRS parameter estimate for each voxel was first converted to a percentage signal change using Featquery, part of the FSL package (Mumford, 2007; Smith, 2006). For each condition (RS and BH), in every voxel the percentage response to the shifted NIRS regressor with the maximum PE value was tabulated. It is meaningful to compare the percentage signal change of these two conditions because the NIRS regressors we used in these two conditions are real measurements of underlying physiological signals, which also directly affect the BOLD signal. This yielded two 3-D maps of maximum signal changes, one for each condition. Furthermore, the ratio between them reflects the real differences in the Δ[tHb] under the two conditions (i.e., they are normalized to the baseline). Fig. 7 shows the results of subject 3, while Fig. 8 shows the results (in the same order as Fig. 7) of averaged data from all 5 subjects. Fig. 7 shows the BOLD signal percentage changes in RS (Fig. 7(a)) and BH (Fig. 7(b)). In both conditions, the signal from the blood vessels, especially the veins, had the largest changes (>20%), which is consistent with the results of the thresholded *z*-statistic map in Fig. 4(b) and (e). The other signal changes are primarily from the gray matter, in both cases with BH having more robust and widespread changes. Fig. 8(a) and (b) shows the same results. This is further illustrated by Fig. 7(d), which shows the histograms of the percentage response to the Δ[tHb] signal of all the voxels in both cases. The mode of the distribution of BH percentage responses is greater than that of RS (2.2%, compared to 1.8%). A similar result is found in Fig. 8(d) with 2.2% in BH compared to 1.0% in RS. It indicates

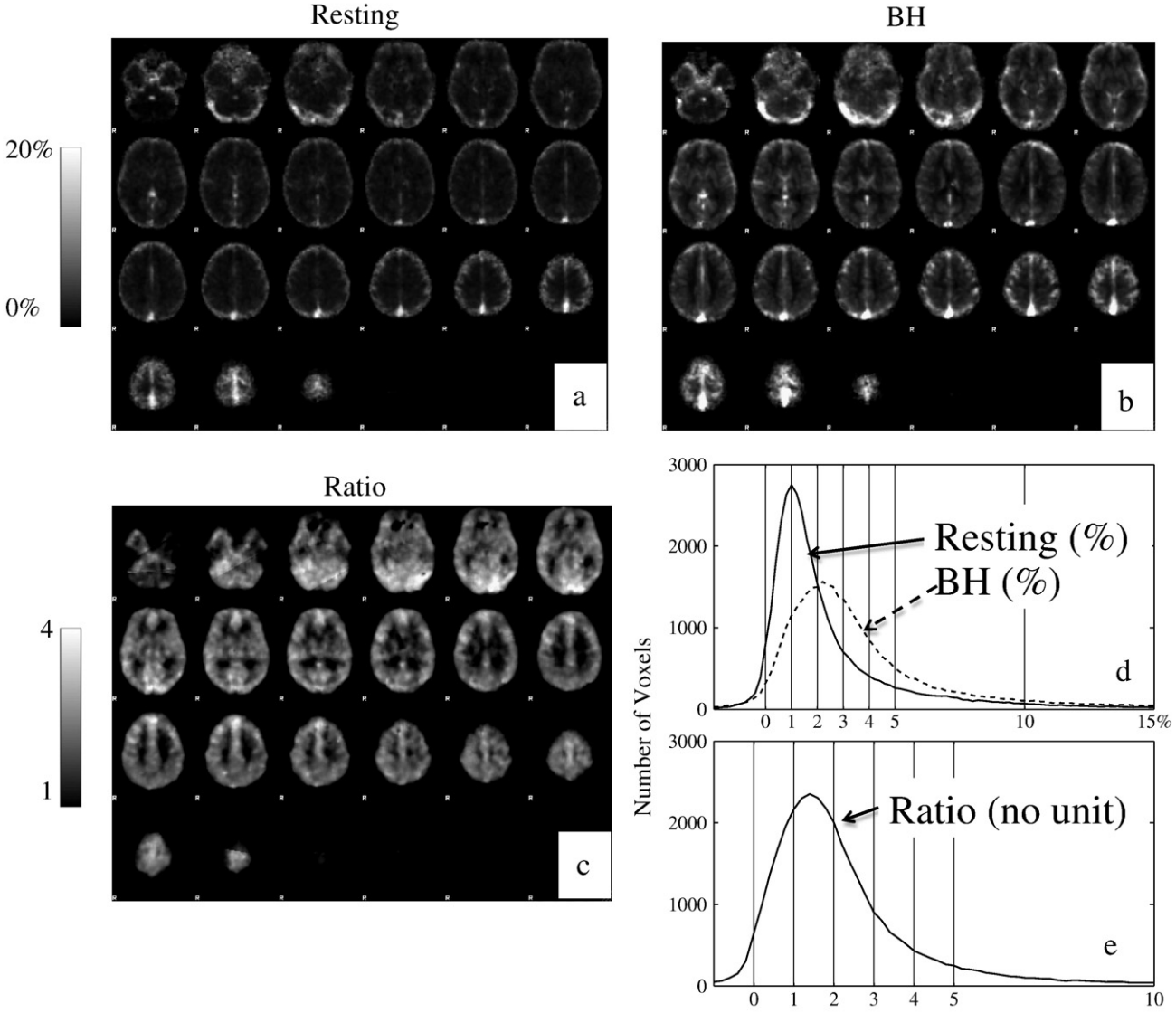

Fig. 8. The maps of averaged BOLD percentage signal change of all subjects for RS (a), BH (b) and the ratio between them (c). (d) Averaged distribution of the voxels based on their signal changes in BH (dotted line) and RS (solid line). (e) Averaged distribution of the voxels based on the ratio between BH and RS calculated at each voxel.

that most voxels have higher BOLD signal changes during BH experiment than the RS. In order to normalize out the "baseline condition," we divide the response map of BH by the map of RS. The resulting normalized CVR maps shown in Fig. 7(c) and Fig. 8(c) demonstrate the following: 1) those voxels with larger percentage response to the Δ[tHb] in the BH than in RS are mostly found in the gray matter; 2) they are evenly spread throughout the brain; 3) the large blood vessels are excluded from the image based on the fact that the signal changes in big blood vessels are similar in both conditions. More interestingly, from Figs. 7(e) and 8(e), where the distribution of the ratio (between BH and RS) is shown, it can be seen that the signal changes from RS to BH are not uniformly increased. Some of the ratio decreases (between 0 and 1 in Figs. 7(e) and 8(e)) indicating smaller changes in BH. As can be seen in Figs. 7(c) and 8(c), the dark area representing the area having these changes (<1) was located mostly in white matter. A combination of factors may be responsible for this observation. First, these voxels are near the ventricular spaces and either the movement or volume change associated with BH may result in some artifactual decrease in signal due to averaging of the vascular ventricular space that moves into the ROI. A second physiological explanation is that the blood flow in the white matter may be decreasing during "stressed situations" (i.e., elevated CO_2 in the blood stream) in order to divert blood to critical brain areas such as the gray matter. This view has some support in the literature (Fern et al., 1998). Further experimentation is ongoing to explore and elucidate these possible mechanisms. There are small numbers of voxels negatively correlated with the NIRS regressor, resulting in negative values in Figs. 7(d and e) and 8(d and e). This could be due to physiological process (i.e., some brain area may inversely correlate with breath holding) or noise.

The method we describe offers a way to compare the BOLD signals quantitatively in two conditions (resting state vs. breath holding). We believe that this method may have clinical utility in assessing vascular reserve longitudinally, in response to drug interventions, in the course of aging, or in disease progression, especially in conditions such as diabetes and cerebrovascular disease that are known to degrade vascular function over time. Further work will be necessary to establish the repeatability and reliability of this measurement for that purpose.

Conclusions

Using concurrently acquired, time-shifted NIRS time courses offers a distinct advantage in the calculation of cerebrovascular reserve maps from breath-holding fMRI data relative to the use of boxcar time courses. The temporally shifted Δ[tHb] time courses obtained from NIRS match the BOLD data much more closely than optimized hemodynamic lag convolved boxcars. Accounting for the varying time shift between different voxels also improves the overall match of the regressors to the data. Moreover, using the shifted NIRS regressors allows calculation of resting state maps with no breath holding, which is not possible with boxcar regressors. This in turn allows us to determine the ratio of the BOLD signal arising from endogenous circulatory variations in the two states, allowing a much more specific measurement of CVR that is less contaminated by variations in baseline blood flow. Future work will use this technique in clinical studies of cerebrovascular diseases and detect abnormalities in cerebrovascular dynamics invoked by the respiratory challenges.

Acknowledgments

The authors would like to thank Dr. Kimberly Lindsey for her extensive comments and suggestions. This work was supported by the National Institutes of Health, Grant No. R21-DA021817and R21-DA027877.

References

Bakker, S.L., de Leeuw, F.E., de Groot, J.C., Hofman, A., Koudstaal, P.J., Breteler, M.M., 1999. Cerebral vasomotor reactivity and cerebral white matter lesions in the elderly. Neurology 52, 578–583.
Brainard, D.H., 1997. The psychophysics toolbox. Spat. Vis. 10, 433–436.
Buxton, R.B., Wong, E.C., Frank, L.R., 1998. Dynamics of blood flow and oxygenation changes during brain activation: the balloon model. Magn. Reson. Med. 39, 855–864.
Chang, C., Thomason, M.E., Glover, G.H., 2008. Mapping and correction of vascular hemodynamic latency in the BOLD signal. Neuroimage 43, 90–102.
Corfield, D.R., Murphy, K., Josephs, O., Adams, L., Turner, R., 2001. Does hypercapnia-induced cerebral vasodilation modulate the hemodynamic response to neural activation? Neuroimage 13, 1207–1211.
Cupini, L.M., Diomedi, M., Placidi, F., Silvestrini, M., Giacomini, P., 2001. Cerebrovascular reactivity and subcortical infarctions. Arch. Neurol. 58, 577–581.
Driver, I., Blockley, N., Fisher, J., Francis, S., Gowland, P., 2010. The change in cerebrovascular reactivity between 3 T and 7 T measured using graded hypercapnia. Neuroimage 51, 274–279.
Emir, U.E., Ozturk, C., Akin, A., 2008. Multimodal investigation of fMRI and fNIRS derived breath hold BOLD signals with an expanded balloon model. Physiol. Meas. 29, 49–63.
Fern, R., Davis, P., Waxman, S.G., Ransom, B.R., 1998. Axon conduction and survival in CNS white matter during energy deprivation: a developmental study. J. Neurophysiol. 79, 95–105.
Goode, S.D., Krishan, S., Alexakis, C., Mahajan, R., Auer, D.P., 2009. Precision of cerebrovascular reactivity assessment with use of different quantification methods for hypercapnia functional MR imaging. AJNR. Am. J. Neuroradiol. 30, 972–977.
Handwerker, D.A., Ollinger, J.M., D'Esposito, M., 2004. Variation of BOLD hemodynamic responses across subjects and brain regions and their effects on statistical analyses. Neuroimage 21, 1639–1651.
Huppert, T.J., Hoge, R.D., Diamond, S.G., Franceschini, M.A., Boas, D.A., 2006. A temporal comparison of BOLD, ASL, and NIRS hemodynamic responses to motor stimuli in adult humans. Neuroimage 29, 368–382.
Jenkinson, M., Smith, S., 2001. A global optimisation method for robust affine registration of brain images. Med. Image Anal. 5, 143–156.
Kastrup, A., Kruger, G., Glover, G.H., Neumann-Haefelin, T., Moseley, M.E., 1999a. Regional variability of cerebral blood oxygenation response to hypercapnia. Neuroimage 10, 675–681.
Kastrup, A., Kruger, G., Neumann-Haefelin, T., Moseley, M.E., 2001. Assessment of cerebrovascular reactivity with functional magnetic resonance imaging: comparison of CO(2) and breath holding. Magn. Reson. Imaging 19, 13–20.
Kastrup, A., Li, T.Q., Glover, G.H., Moseley, M.E., 1999b. Cerebral blood flow-related signal changes during breath-holding. AJNR. Am. J. Neuroradiol. 20, 1233–1238.
Kozera, G.M., Wolnik, B., Kunicka, K.B., Szczyrba, S., Wojczal, J., Schminke, U., Nyka, W.M., Bieniaszewski, L., 2009. Cerebrovascular reactivity, intima-media thickness, and nephropathy presence in patients with type 1 diabetes. Diabetes Care 32, 878–882.
Lee, A.T., Glover, G.H., Meyer, C.H., 1995. Discrimination of large venous vessels in time-course spiral blood-oxygen-level-dependent magnetic-resonance functional neuroimaging. Magn. Reson. Med. 33, 745–754.
Li, T.Q., Kastrup, A., Takahashi, A.M., Moseley, M.E., 1999. Functional MRI of human brain during breath holding by BOLD and FAIR techniques. Neuroimage 9, 243–249.
Liu, H.L., Huang, J.C., Wu, C.T., Hsu, Y.Y., 2002. Detectability of blood oxygenation level-dependent signal changes during short breath hold duration. Magn. Reson. Imaging 20, 643–648.
Lythgoe, D.J., Williams, S.C., Cullinane, M., Markus, H.S., 1999. Mapping of cerebrovascular reactivity using BOLD magnetic resonance imaging. Magn. Reson. Imaging 17, 495–502.
MacIntosh, B.J., Klassen, L.M., Menon, R.S., 2003. Transient hemodynamics during a breath hold challenge in a two part functional imaging study with simultaneous near-infrared spectroscopy in adult humans. Neuroimage 20, 1246–1252.
Magon, S., Basso, G., Farace, P., Ricciardi, G.K., Beltramello, A., Sbarbati, A., 2009. Reproducibility of BOLD signal change induced by breath holding. Neuroimage 45, 702–712.
Mandell, D.M., Han, J.S., Poublanc, J., Crawley, A.P., Stainsby, J.A., Fisher, J.A., Mikulis, D.J., 2008. Mapping cerebrovascular reactivity using blood oxygen level-dependent MRI in Patients with arterial steno-occlusive disease: comparison with arterial spin labeling MRI. Stroke 39, 2021–2028.
Matcher, S.J., 1994. Use of the water absorption spectrum to quantify tissue chromophore concentration changes in near-infrared spectroscopy. Phys. Med. Biol. 39, 177–196.
Miezin, F.M., Maccotta, L., Ollinger, J.M., Petersen, S.E., Buckner, R.L., 2000. Characterizing the hemodynamic response: effects of presentation rate, sampling procedure, and the possibility of ordering brain activity based on relative timing. Neuroimage 11, 735–759.
Mumford, J., A Guide to Calculating Percent Change with Featquery.
Murphy, K., Harris, A.D., Wise, R.G., 2011. Robustly measuring vascular reactivity differences with breath-hold: normalising stimulus-evoked and resting state BOLD fMRI data. Neuroimage 54, 369–379.
Okamoto, M., Dan, H., Sakamoto, K., Takeo, K., Shimizu, K., Kohno, S., Oda, I., Isobe, S., Suzuki, T., Kohyama, K., Dan, I., 2004. Three-dimensional probabilistic anatomical cranio-cerebral correlation via the international 10–20 system oriented for transcranial functional brain mapping. Neuroimage 21, 99–111.
Pindzola, R.R., Balzer, J.R., Nemoto, E.M., Goldstein, S., Yonas, H., 2001. Cerebrovascular reserve in patients with carotid occlusive disease assessed by stable xenon-enhanced ct cerebral blood flow and transcranial Doppler. Stroke 32, 1811–1817.
Sassaroli, A., de, B.F.B., Tong, Y., Renshaw, P.F., Fantini, S., 2006. Spatially weighted BOLD signal for comparison of functional magnetic resonance imaging and near-infrared imaging of the brain. Neuroimage 33, 505–514.

Smith, S.M., 2006. Featquery—FEAT results interrogation.
Smith, S.M., Jenkinson, M., Woolrich, M.W., Beckmann, C.F., Behrens, T.E., Johansen-Berg, H., Bannister, P.R., De Luca, M., Drobnjak, I., Flitney, D.E., Niazy, R.K., Saunders, J., Vickers, J., Zhang, Y., De Stefano, N., Brady, J.M., Matthews, P.M., 2004. Advances in functional and structural MR image analysis and implementation as FSL. Neuroimage 23 (Suppl 1), S208–S219.
Strangman, G., Culver, J.P., Thompson, J.H., Boas, D.A., 2002. A quantitative comparison of simultaneous BOLD fMRI and NIRS recordings during functional brain activation. Neuroimage 17, 719–731.
Thomason, M.E., Burrows, B.E., Gabrieli, J.D., Glover, G.H., 2005. Breath holding reveals differences in fMRI BOLD signal in children and adults. Neuroimage 25, 824–837.
Tong, Y., Frederick, B.D., 2010. Time lag dependent multimodal processing of concurrent fMRI and near-infrared spectroscopy (NIRS) data suggests a global circulatory origin for low-frequency oscillation signals in human brain. Neuroimage 53, 553–564.
Toronov, V., Webb, A., Choi, J.H., Wolf, M., Michalos, A., Gratton, E., Hueber, D., 2001. Investigation of human brain hemodynamics by simultaneous near-infrared spectroscopy and functional magnetic resonance imaging. Med. Phys. 28, 521–527.
van der Kouwe, A.J., Benner, T., Salat, D.H., Fischl, B., 2008. Brain morphometry with multiecho MPRAGE. Neuroimage 40, 559–569.
van der Zande, F.H., Hofman, P.A., Backes, W.H., 2005. Mapping hypercapnia-induced cerebrovascular reactivity using BOLD MRI. Neuroradiology 47, 114–120.
Vernieri, F., Pasqualetti, P., Passarelli, F., Rossini, P.M., Silvestrini, M., 1999. Outcome of carotid artery occlusion is predicted by cerebrovascular reactivity. Stroke 30, 593–598.
Vernieri, F., Tibuzzi, F., Pasqualetti, P., Rosato, N., Passarelli, F., Rossini, P.M., Silvestrini, M., 2004. Transcranial Doppler and near-infrared spectroscopy can evaluate the hemodynamic effect of carotid artery occlusion. Stroke 35, 64–70.
Vernooij, M.W., van der Lugt, A., Ikram, M.A., Wielopolski, P.A., Vrooman, H.A., Hofman, A., Krestin, G.P., Breteler, M.M., 2008. Total cerebral blood flow and total brain perfusion in the general population: the Rotterdam Scan Study. J. Cereb. Blood Flow Metab. 28, 412–419.
Woolrich, M.W., Ripley, B.D., Brady, M., Smith, S.M., 2001. Temporal autocorrelation in univariate linear modeling of FMRI data. Neuroimage 14, 1370–1386.
Yezhuvath, U.S., Lewis-Amezcua, K., Varghese, R., Xiao, G., Lu, H., 2009. On the assessment of cerebrovascular reactivity using hypercapnia BOLD MRI. NMR Biomed. 22, 779–786.
Yezhuvath, U.S., Uh, J., Cheng, Y., Martin-Cook, K., Weiner, M., Diaz-Arrastia, R., van Osch, M., Lu, H., 2010. Forebrain-dominant deficit in cerebrovascular reactivity in Alzheimer's disease. Neurobiol. Aging.
Ziyeh, S., Rick, J., Reinhard, M., Hetzel, A., Mader, I., Speck, O., 2005. Blood oxygen level-dependent MRI of cerebral CO2 reactivity in severe carotid stenosis and occlusion. Stroke 36, 751–756.